VSP *J. Adhesion Sci. Technol. (2011)* DOI:10.1163/156856111X600244

Journal of ADHESION SCIENCE and TECHNOLOGY
brill.nl/jast

Electrowetting on Flexible Substrates

H. You and A. J. Steckl *

Nanoelectronics Laboratory, Department of Electrical and Computer Engineering, University of Cincinnati, Cincinnati, Ohio 45221-0030, USA

Abstract

Electronic readers that use rugged flexible substrates potentially offer very attractive characteristics (low-cost processing, lightweight, mechanical flexibility, etc.) and could expand the explosive growth of e-reader devices. In this paper, we demonstrate electrowetting (EW) devices fabricated on flexible substrates, including paper, polymers (plastics), and metal foils and sheets. EW devices on some of the flexible substrates exhibit characteristics very close to those of conventional EW devices on glass substrates. Prototypes of flexible EW arrays on plastic substrates are demonstrated to switch reversibly by applying a low voltage difference (20 V). The array operation is maintained even when the display is mechanically flexed. These results indicate the promise of flexible EW devices for mobile and other devices, including video rate flexible e-paper.

Keywords

Electrowetting, flexible substrate, e-paper, e-reader

1. Introduction

New applications for electronics require systems that can be fitted into non-planar forms, or can be folded for packing or storage and unfolded for use. Flexible displays are expected to play an increasing role in many applications, ranging from newspaper-like displays [1, 2], radio-frequency identification (RFID) tags [3], displays worn on the body, toys, packaging [4, 5], and biomedical devices [6]. Technologies based on organic semiconductors [7, 8], roll to roll printed polymers [9, 10], and carbon nanotubes [11] have contributed to the development of flexible electronics. For portable devices, the concern for low power consumption and the ability to work well in bright lighting conditions point to the need for reflective display technologies that do not require backlighting and have enough brightness in the outdoor condition. Many of the e-reader products recently commercially introduced use electrophoretic displays (EPDs) [12]. However, other technologies are also being investigated because EPDs are fundamentally monochrome and do not have the speed required for video display.

* To whom correspondence should be addressed. E-mail: a.steckl@uc.edu

 DOI:10.1163/156856111X600244

Electrowetting (EW) [13] provides another approach for control of light. The interaction of light with an EW structure (i.e., the combination of absorption, transmission, and reflection) is controlled by the motion of two immiscible liquids (one clear and one colored) under the influence of an electric field [14]. The EW light valve approach is quite versatile, leading to many important applications [15]. In many of these applications, the EW switching speed in the millisecond range [16] is an important asset, enabling video-rate operation (∼30 frames/s). Currently, the major application of EW technology is in the field of flat panel displays on fixed substrates (glass) [17]. EW displays with multiple colors have been achieved without the use of color filters using a vertical stack structure also on a glass substrate [18]. Other important applications of EW technology include lenses with electronic focus [19, 20], microfluidic devices [21, 22], and liquid-state transistors [23].

Recently, EW operation on paper substrates was shown [24] to have switching speeds comparable to those on glass substrates. This has increased the interest in flexible EW displays. In this paper, EW operation on flexible substrates of various materials (paper, plastic, metal) is discussed and EW display prototypes are demonstrated.

2. Fabrication Process

Diagrams of EW structures on flexible substrates are shown in Fig. 1. EW operation on a completely rolled flexible substrate is illustrated in Fig. 1(a) [24]. In this case the structure consists of a ground electrode, a dielectric layer, and a fluoropolymer layer. The structure for an array of EW devices on a flexible substrate is shown in Fig. 1(b). For the array devices on plastic substrates, a 10-μm-high hydrophilic grid uses epoxy-based negative photoresist (SU-8 2010, MicroChem, Newton, MA) to confine the color oil layer, which was formulated by dissolving non-polar dyes (Keystone Co., Chicago, IL) in dodecane (Acros Organics, Thermo Fisher Scientific, Morris Plains, NJ). The top layer that seals the array is made from poly(dimethylsiloxane) (PDMS).

Several types of materials were investigated for use as flexible substrates for EW devices: paper, polymers, metals. Specific materials were selected from each group based on the requirements of the fabrication process and device operation. For paper substrates, glassine paper, Kromekote paper and Sappi paper (Sappi Fine Paper, Westbrook, ME) were used as the substrate. The metal electrode deposited on the paper substrate was either transparent indium tin oxide (ITO) or reflective Cu. Details of the fabrication process on paper substrates have been previously described [24].

For the EW array structure on plastic, poly(ethylene terephthalate) (PET) polymer was utilized as the substrate. The PET substrate had a thickness of 175 μm. A 200 nm transparent ITO electrode was deposited on the polymer substrate followed by the deposition of a 1 μm organic dielectric (parylene) layer. The top layer is the hydrophobic insulator FluoroPel™ (PFC1601V, Cytonix Corporation,

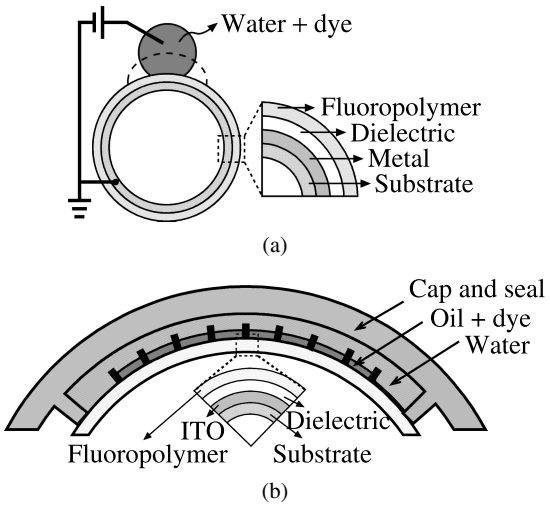

Figure 1. Diagrams of electrowetting on curved surfaces: (a) cross section of device structure for EW of water droplet; (b) cross section of pixel array for competitive EW of water and oil.

Beltsville, MD). A 1% Fluoropel solution in fluorosolvent was spin-coated at 3000 rpm for 30 s, forming a ∼40 nm film. After spin coating, a subsequent annealing at 180°C for 30 min optimizes the Fluoropel adhesion. The resulting Fluoropel film can reach a surface energy of ∼14–16 mJ/m^2. For the devices on metal substrates, the same dielectric and fluoropolymer deposition processes were used.

Alkanes were used for the oil in the structures. Alkanes are non-polar and do not dissolve in water. For the experiments described in this paper, dodecane was utilized.

Demonstrations of EW action on flexible substrates made from different materials are shown in Fig. 2, where the substrates are bent to form varying degrees of curvature. Figure 2(a) and (b) [24] show deionized (DI) water droplets placed on EW structures on curved paper substrates with ITO and Cu electrodes, respectively. Figure 2(c) and (d) show deionized (DI) water droplets placed on EW structures on curved Cu foil and steel sheet, respectively. The left and right droplets show the high contact angle (CA) typical of aqueous droplets on hydrophobic surfaces. A wire is inserted into the middle droplet, through which external voltage is applied. The EW effect results in an observable CA change. The inserts in Fig. 2 allow easy observation of the shape of the droplet with applied voltage (right) and at zero bias (left).

For the array devices, Cytop (CTL-809M, Asahi, Japan) was used as the fluoropolymer. After spin coating, the Cytop layer was soft baked at ∼70°C for ∼8 min. Next, the negative photoresist SU-8 was spin-coated at 3500 rpm for 2 min, forming a ∼10-μm-thick film. The photolithography process consists of the following steps: resist soft baking at 65°C and 95°C for 3 min each, 365 nm UV exposure with an i-line mask aligner (EVG 420, Electronic Visions Inc., Tempe, AZ) with

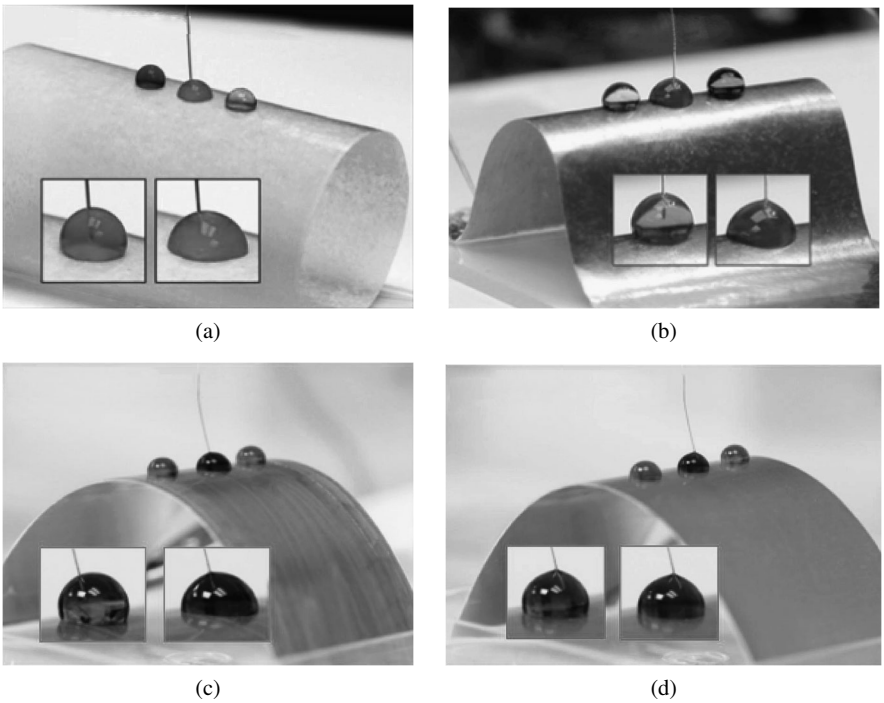

Figure 2. Photographs of electrowetting on various flexible substrates: (a) ITO-coated paper; (b) Cu-coated paper; (c) Cu foil on steel sheet; (d) steel sheet.

an intensity of ∼10 mW/cm^2 for 14 s, post exposure bake (PEB) at 95°C for 3 min, development using SU-8 developer for 40 s, followed by isopropyl alcohol rinse for 10 s. Then, the sample was baked at 150°C for 30 min to improve the SU-8 adhesion to the hydrophobic insulator. The oil dispensing is accomplished by the self-assembled dosing technique [25]. The thickness of the oil film can be controlled by the dip speed. Then, the devices are aligned and sealed inside a DI water container with a PDMS cover resulting in the final assembly shown in Fig. 1(b).

The CA was measured with the VCA Optima XE (Advanced Surface Technology, Billerica, MA) system. The paper device was immersed in an oil container and a 3 µl DI water droplet was injected for CA measurement. The external bias was applied to the droplet through a wire connected to a function generator (AFG310, SONY Tektronix, Japan) and a voltage amplifier (F10AD, FLC Electronics, Sweden).

3. Results and Discussion

The EW effect on polymer substrates was investigated by measuring the CA of DI water droplets. Figure 3 compares CA change on PET and glass substrates as a function of applied DC voltage. The initial contact angles of 5 µl DI water droplets on the Cytop surface were 110° and 112° for glass and PET substrates, respectively.

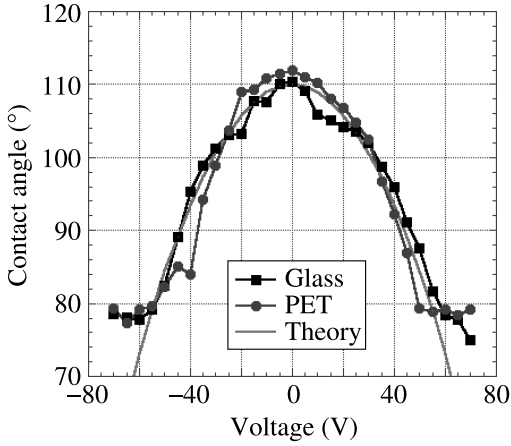

Figure 3. Comparison of water contact angle in air *versus* voltage for glass (rigid) and PET (flexible) substrates. The continuous line gives the theoretical contact angles based on the coating thickness and dielectric constant: 40 nm Cytop on top of 1 μm parylene C.

Over a considerable voltage range the experimental CA data are in agreement with values calculated from EW theory:

$$\cos\theta(V) = \cos\theta_0 - \frac{\varepsilon_0\varepsilon_1\varepsilon_2 V^2}{2(\varepsilon_1 d_2 + \varepsilon_2 d_1)\gamma_{\mathrm{W}}}, \tag{1}$$

where γ_{W} is the surface tension of DI water surrounded by either oil (γ_{WO}) or air (γ_{WA}); ε_1 and ε_2 are the relative dielectric constants for the parylene and Cytop layers, respectively; d_1 and d_2 are the thicknesses of the parylene and Cytop layer dielectric layers, respectively; θ_0 is the CA at zero bias, and V is the applied DC voltage. The contact angles on glass and PET devices with 1-μm-thick parylene dielectric layer generally followed the calculated values with applied voltage, gradually decreasing to 81° and 79°, respectively, as the voltage increased to 55 V. For many materials systems used in EW structures, CA saturation is observed at higher voltages. This deviation from theoretically expected behavior is generally associated with charge trapping in or on the insulator and with surface quality. The contact angles on both glass and PET devices started to saturate at ∼60 V. As can be seen, the EW device on the PET substrate exhibited characteristics very similar to the device on conventional glass substrate.

A flexible EW display device consisting of a 45 × 21 pixel array with 300 μm × 900 μm pixel area is shown in Fig. 4. Oil with red dye is used for visualization purposes. The device is photographed while being manually flexed. The left and right photographs show the array at zero voltage (OFF state — oil covering pixels) and −20 V voltage (ON state — oil displaced), respectively. The array is fully operational in both OFF and ON states while being bent in a curved shape. In addition, the array was also found to be fully functional while flexed in either the OFF or ON state. Varying the applied voltage controls the oil coverage in the pixel which

(a) (b)

Figure 4. EW operation on flexible pixel array with transparent plastic substrate (PET) and top cover (PDMS): (a) voltage off; (b) voltage on.

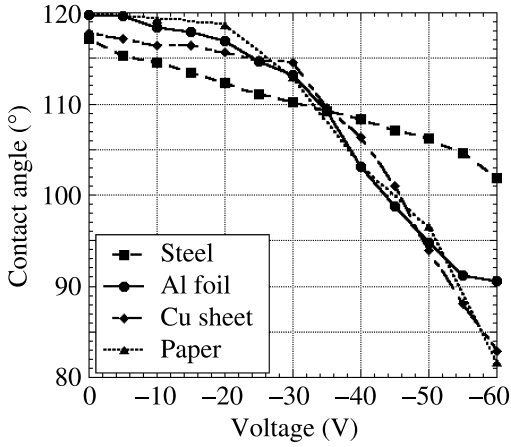

Figure 5. Comparison of water contact angle in air *versus* voltage for various flexible substrates.

determines the extent of the oil-free 'open' area. In turn, this enables gray scale operation of the display. The EW reflective display specifications are maintained even when the display is mechanically flexed.

The EW effect on different flexible substrates, including the paper, steel sheet, aluminum and copper foils, was evaluated by measuring the CA of DI water droplets as a function of the applied DC voltage. The measurements used 3 μl DI water droplets on an EW structure with a 1-μm-thick parylene C dielectric layer and a 40 nm Fluoropel film. In general, the maximum voltage utilized was 60 V in order to prevent dielectric breakdown, which for these devices typically occurred at ∼70 V. As shown in Fig. 5, the initial CAs on the Fluoropel surface were nearly identical at ∼120° for paper, steel sheet, Al and Cu foil substrates. The CA of all the devices monotonically decreased with increasing applied voltage from 0 to −60 V. The pa-

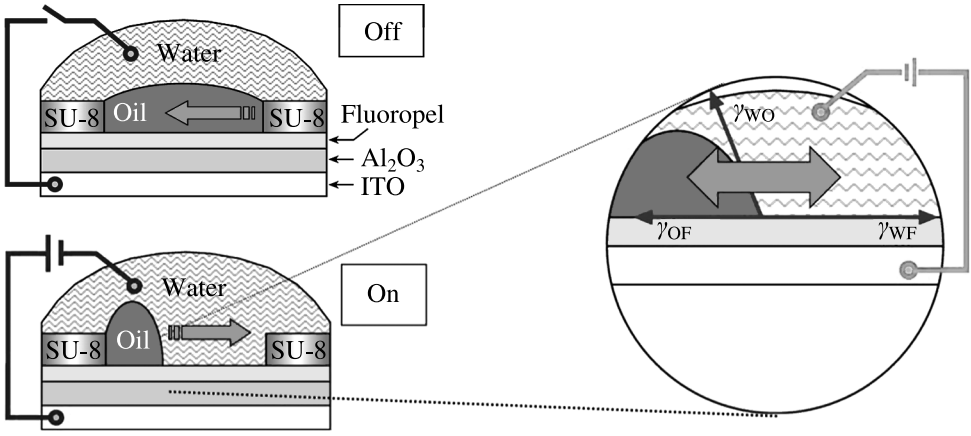

Figure 6. Diagrams illustrating the effect of water/oil interfacial tension during turn-on (wetting) and turn-off (dewetting) in EW devices.

Table 1.
Driving force for turn-on and turn-off processes in EW devices. Driving forces: electrical (F_E), interfacial tension (F_γ), friction (F_F)

EW state	Driving force	Water–oil interfacial tension (γ_{WO})
Off → On	$F_E - F_\gamma - F_F$	want low
On → Off	$F_\gamma - F_F$	want high

per, Cu and Al foil devices all show a relatively large CA change (∼30–40°), with the paper substrate producing the largest change (∼38°). On the other hand, the steel sheet device exhibited a relatively small CA change (∼15°). This is possibly due to the presence of an insulator layer on the as-received steel sheet producing a larger total dielectric layer thickness.

The switching speed of EW devices is directly related to the rate with which the water replaces oil under the influence of the applied voltage, which in turn is determined by the rate of the change in contact angle. As illustrated in Fig. 6, the net driving force during turn-on (wetting) is given by the difference between the water advancing effect of the electric field (F_E) and the retarding effect (F_γ) of the oil–water interfacial tension (γ_{WO}) and oil–solid interface friction (F_F). Therefore, a relatively low (but obviously not too low) value of γ_{WO} is desirable. In contrast, during turn-off (dewetting) the interfacial tension is the advancing component of the driving force. In this case, a high value of γ_{WO} will result in a shorter turn-off time. In both cases, having a very smooth solid surface will minimize the surface friction and decrease the switching times. This trade-off between turn-on and turn-off times is summarized in Table 1.

Table 2.
Switching time (ms) of water droplet in oil for wetting (turn-on) and dewetting (turn-off) for glass and various flexible substrates (defined as the time it takes to complete 80% of the optical modulation)

	Thickness (μm)	Wetting time (ms)	Dewetting time (ms)	Reference
Glass	1100	15	17	[24]
Glassine paper	45	28	40	[24]
Kromekote paper	235	28	29	[24]
Sappi paper	180	19	19	[24]
Steel sheet	250	15	34	this work
Copper foil	60	15	27	this work
Aluminum foil	15	14	27	this work

The CA of 3 μl DI water droplets in oil ambient was measured as a function of time as a 40 V pulse with fast rise/fall times (∼2 ns) was applied to the droplet. The CA pulse responses (defined as the time it takes to complete 80% of the optical modulation) for wetting and dewetting processes for EW devices on glass, several types of paper, steel sheet, copper and aluminum foils are summarized in Table 2. All EW structures used the same dielectric layers and thicknesses. The wetting/dewetting times for the glass and paper substrates have been previously reported [24]. As expected, the glass substrate device produced the shortest switching times for both wetting (15 ms) and dewetting (17 ms). The best results on paper substrates (Sappi) showed only slightly longer wetting/dewetting times of 19/19 ms. Interestingly, the structures on the metallic substrates produced a wetting time almost equal to that on glass. The dewetting times of these substrates were longer that on glass. This effect is probably due to the rougher surfaces that affect the friction between the oil and the substrates. The rate of change in diameter for a water droplet in oil is known to be proportional to interfacial tension between the two fluids and inversely proportional to the coefficient of friction [26]. For the experiments reported here, the droplet volume of 3 μl results in a droplet diameter of ∼1.8 mm on the fluoropolymer surface. Droplet wetting and dewetting times are known to be linearly related to the droplet diameter [27], with values of ∼10–20 ms reasonable for our droplet size and experimental conditions. It needs to be mentioned that CA hysteresis can also affect the wetting/dewetting times.

The same switching time imbalance was observed with the rougher paper substrate (glassine). This indicates that surfaces with improved quality (smoothness) for metal substrates along with paper and plastic have a good potential for EW-based flexible displays.

4. Summary

The operation of EW structures on several types of flexible substrates (paper, plastic and metal) has been demonstrated, indicating the feasibility of using these

substrates as a cheap and flexible option for EW-based e-paper displays. Their relatively fast switching speed (of the order of a few tens of milliseconds) is very promising for video display applications. EW display prototypes on plastic substrates have been shown to operate even when the units are mechanically flexed.

Acknowledgements

Support for this project by the National Science Foundation and the Raytheon Company is gratefully acknowledged. The authors appreciate many useful technical discussions on EW with members of the Nanoelectronics Laboratory and Novel Devices Laboratory at the University of Cincinnati.

References

1. J. A. Rogers, Z. Bao, K. Baldwin, A. Dodabalapur, B. Crone, V. R. Raju, V. Kuck, H. Katz, K. Amundson, J. Ewing and P. Drzaic, *Proc. Natl. Acad. Sci. U.S.A.* **98**, 4835 (2001).
2. G. H. Gelinck, H. E. A. Huitema, E. Van Veenendaal, E. Cantatore, L. Schrijnemakers, J. B. P. H. Van der Putten, T. C. T. Geuns, M. Beenhakkers, J. B. Giesbers, B. H. Huisman, E. J. Meijer, E. M. Benito, F. J. Touwslager, A. W. Marsman, B. J. E. Van Rens and D. M. De Leeuw, *Nature Mater.* **3**, 106 (2004).
3. V. Subramanian, J. M. J. Frechet, P. C. Chang, D. C. Huang, J. B. Lee, S. E. Molesa, A. R. Murphy, D. R. Redinger and S. K. Volkman, *Proc. IEEE* **93**, 1330 (2005).
4. S. Park and S. Jayaraman, *MRS Bull.* **28**, 585 (2003).
5. M. Hamedi, R. Forchheimer and O. Inganas, *Nature Mater.* **6**, 357 (2007).
6. W. W. Wang, G. K. Knopf and A. S. Bassi, *IEEE Trans. Nanobioscience* **7**, 249 (2008).
7. S. R. Forrest, *Nature* **428**, 911 (2004).
8. F. Garnier, R. Hajlaoui, A. Yassar and P. Srivastava, *Science* **265**, 1684 (1994).
9. D. Y. Chung, J. S. Huang, D. D. C. Bradley and A. J. Campbell, *Org. Electron.* **11**, 1088 (2010).
10. M. Berggren, D. Nilsson and N. D. Robinson, *Nature Mater.* **6**, 3 (2007).
11. J. A. Rogers, *Nature Nano.* **3**, 254 (2008).
12. B. Comiskey, J. D. Albert, H. Yoshizawa and J. Jacobson, *Nature* **394**, 253 (1998).
13. F. Mugele and J. C. Baret, *J. Phys.: Condens. Matter* **17**, R705 (2005).
14. C. Quilliet and B. Berge, *Curr. Opin. Colloid Interface Sci.* **6**, 34 (2001).
15. R. Shamai, D. Andelman, B. Berge and R. Hayes, *Soft Matter.* **4**, 38 (2008).
16. J. Heikenfeld and A. J. Steckl, *Appl. Phys. Lett.* **86**, 151121 (2005).
17. R. A. Hayes and B. J. Feenstra, *Nature* **425**, 383 (2003).
18. H. You and A. J. Steckl, *Appl. Phys. Lett.* **97**, 023514 (2010).
19. B. Berge and J. Peseux, *Euro. Phys. J. E* **3**, 159 (2000).
20. S. Kuiper and B. H. W. Hendriks, *Appl. Phys. Lett.* **85**, 1128 (2004).
21. J. Lee, H. Moon, J. Fowler, T. Schoellhammer and C. J. Kim, *Sensors Actuators A* **95**, 259 (2002).
22. P. Paik, V. K. Pamula, M. G. Pollack and R. B. Fair, *Lab on a Chip* **3**, 28 (2003).
23. D. Y. Kim and A. J. Steckl, *Appl. Phys. Lett.* **90**, 043507 (2007).
24. D. Y. Kim and A. J. Steckl, *ACS Appl. Mater. Interfaces* **2**, 3318 (2010).
25. B. Sun, K. Zhou, Y. Lao, J. Heikenfeld and W. Cheng, *Appl. Phys. Lett.* **91**, 011106 (2007).
26. C. Decamps and J. De Coninck, *Langmuir* **16**, 10150 (2000).
27. Z. L. Wan, H. Zeng and A. Feinerman, *ASME Trans. J. Fluid. Eng.* **129**, 388 (2007).